Instability order and the selection mechanism of self-similar blowup in the Sabra shell model, and a family-type dichotomy of blowup universality

Carles Marín
Independent Researcher

May 25, 2026

Abstract

The inviscid Sabra shell model of turbulence blows up in finite time through a self-similar profile that was recently shown to be non-unique: an infinite family of N-bump profiles coexists with the attracting one-bump profile, leaving open (i) the linear stability of the family and (ii) the selection mechanism that makes the one-bump profile universal [Campolina–Simonnet–Thalabard, 2025]. We compute the one-bump profile to machine precision, derive its renormalized-time stability operator, and show its spectrum is stable (instability order 0) up to the trivial t^*-shift, translation, and a golden-ratio phase mode arising from the Sabra phase symmetry (a Fibonacci recurrence). Treating the N-bump profile as a weakly-coupled bound state of one-bump pulses, we show by a pulse-interaction computation that its *instability order equals* $N-1$: only the one-bump profile is a stable attractor, which *explains the observed selection*. We then test the recently proposed rate–instability-order universality law [unstable-singularities program, 2025] and find it does *not* transfer to Sabra: its exponents *cluster* (multi-pulse accumulation) rather than *spread* (reciprocal-affine). This motivates a family-type dichotomy of self-similar blowup — *distinct-profile/intrinsic-instability* families (rate spreads) versus *multi-pulse/interaction* families (rate clusters) — with a sharp discriminator of the instability count: the internal *phase freedom* of the pulse, which turns the real-symmetric interaction (rigid pulses, Sabra; order $N-1$) into a complex Toda chain (phase pulses, nonlinear Schrödinger / Ginzburg–Landau multibumps; phase-dependent order).

1 Introduction

Motivation. Whether solutions of the 3D incompressible Euler and Navier–Stokes equations can develop a finite-time singularity from smooth data is among the central open problems of mathematical fluid dynamics (the Navier–Stokes regularity question is a Clay Millennium Problem). Rigorous and computer-assisted progress on the inviscid/boundary side — Luo–Hou [14], Elgindi [15], Chen–Hou [12, 13] — and a recent wave of machine-learning discoveries of unstable singularities [3] have made the *structure and stability* of self-similar blowup profiles a focal point: which profile is realised, how many unstable directions it carries, and whether such data obey universal laws. Beyond regularity, blowup is conjectured to be the engine of the bursty, intermittent statistics of turbulence [6, 18, 19]. Shell models are the standard tractable arena in which these questions can be answered completely, and then used to guide the genuine PDE problem.

Background. Shell models reduce the Navier–Stokes/Euler cascade to a chain of complex amplitudes u_n on a geometric sequence of scales $k_n = \lambda^n$, retaining the quadratic energy-conserving

nonlinearity and the inertial cascade while being numerically tractable. The Sabra model [1] is the standard such testbed and is conjectured to blow up in finite time through a self-similar profile. Campolina, Simonnet and Thalabard [2] recently established that this blowup is *non-unique*: alongside the attracting one-bump profile (exponent $x_1 \approx 0.281$) there exists a family of N-bump profiles with exponents $x_N \geq x_1$. They left two questions open: the linear stability of the family, and the selection mechanism that singles out the one-bump profile observed from generic data.

Contributions. We resolve both questions for Sabra and place the result in a cross-equation context.

Result 1 (Selection via instability order)**.** The N-bump profile has instability order $N-1$; the one-bump profile (order 0) is the unique stable attractor, which explains the observed selection.

Result 2 (Family-type dichotomy and a phase discriminator)**.** Self-similar blowup families split into a *distinct-profile* class (intrinsic instabilities; exponents spread, obeying the reciprocal-affine rate–order law of [3]) and a *multi-pulse* class (interaction instabilities; exponents cluster). Within the multi-pulse class the instability count is governed by the pulse's internal phase freedom: rigid (real) pulses give a real-symmetric interaction and order $N-1$, while phase pulses give a complex Toda chain and a phase-dependent order.

Calibration. Throughout, we distinguish [computed] (machine-precision, this work), [known] (published), and [synthesis] (our organizing framework, well-supported but not a theorem). Result 1's *count* $N-1$ is rigorous (a symmetry argument, cf. [7]); that all $N-1$ are *unstable* is [computed] for Sabra and is *not* universal — [7] shows the unstable count ranges in $\{0,\ldots,N-1\}$ system-by-system. Result 2 is [synthesis].

Relation to prior work. [2] discovered the N-bump family, derived the Hopf bifurcation (our Eq. (4) reproduces their Theorem 1), and reported *qualitatively* that the one-bump profile is stable and multi-bumps appear unstable, via machine-learning optimisation; they did not compute a spectrum, an instability order, or a selection mechanism. [4, 5] developed the renormalisation and bifurcation picture of shell-model blowup, and [7] the general theory of multiple-pulse stability that we invoke. The rate–instability-order law for distinct-profile families is [3]; the stability of NLS/Ginzburg–Landau soliton trains (our multi-pulse exemplars) is classical via the complex Toda chain [11, 8, 9]. Our new contributions are the quantitative order law $N-1$ and selection mechanism for Sabra, the pulse-interaction method (instability order without resolving the saddle orbit), and the unifying family-type dichotomy with its phase discriminator.

Validation. Every step carries an internal check: the inviscid invariants E, H are conserved to $\sim 10^{-13}$ (correctness of (1)); the connecting-orbit residual reaches $\sim 10^{-16}$ and $x = 0.2842,\ 0.2824,\ 0.2818$ for grid refinement $m = 4, 6, 8$ (converging to ≈ 0.281); the translation zero-mode of the stability operator is recovered; the Hopf exponent is obtained by two independent routes (closed form and a truncated hierarchy, agreeing to four digits); and the golden-ratio phase mode is confirmed both by its predicted value and by eigenvector correlation (1.0000).

2 Model and self-similar profile

What is the shape of the blowup, and how precisely can we pin it down? The inviscid Sabra model ($\lambda = 2$, $g = 1$, $c = -\lambda^{-g} = -\frac{1}{2}$, $k_n = \lambda^n$) is

$$\frac{du_n}{dt} = ik_n\big[\lambda\, u_{n+2}u^*_{n+1} - (1+c)\, u_{n+1}u^*_{n-1} - \tfrac{c}{\lambda}\, u_{n-1}u_{n-2}\big], \tag{1}$$

conserving $E = \sum |u_n|^2$ and helicity $H = \sum(-1)^n k_n |u_n|^2$. With the self-similar ansatz $u_n(t) = -i(t^*-t)^{x/(1-x)}\,\mathcal{U}(\eta_n)$, $\eta_n = (t^*-t)^{1/(1-x)}k_n$, the factor $-i$ renders the profile $\mathcal{U}$ *real* (the conjugates in (1) are absorbed), giving the profile equation

$$x\,\mathcal{U}(\eta_n) + \eta_n\,\mathcal{U}'(\eta_n) = (1-x)\,\eta_n\big[\lambda\,\mathcal{U}_{n+2}\mathcal{U}_{n+1} - (1+c)\,\mathcal{U}_{n+1}\mathcal{U}_{n-1} + c\lambda^{-1}\mathcal{U}_{n-1}\mathcal{U}_{n-2}\big]. \tag{2}$$

In the autonomous variable $s = (1-x)\log\eta$, $W(s) = e^s\mathcal{U}$, with shift $\delta = (1-x)\log\lambda$,

$$W'(s) = W + \lambda^{-2}W_{2\delta}W_\delta - (1+c)W_\delta W_{-\delta} + c\lambda^2 W_{-\delta}W_{-2\delta}, \qquad W_{j\delta}(s) = W(s+j\delta). \tag{3}$$

We solve (3) by a connecting-orbit Newton method on a grid of spacing $d = (1-x)\log\lambda/m$, so the eigenvalue x enters *through the shift* (exact integer index shifts $\pm m, \pm 2m$) rather than as a prefactor. This converges to machine precision (residual $\sim 6\times10^{-17}$), with $x \to 0.281$ under refinement and robustly independent of the seed (Fig. 1A). [computed]

Constant fixed point and Hopf. Equation (3) has a constant fixed point $\mathcal{W}^* = -1/K$, $K = \lambda^{-2} - (1+c) + c\lambda^2$, whose linearization yields a closed-form Hopf exponent

$$x_{\mathrm{Hopf}} = 1 - \frac{(\lambda^2-1)(1-c\lambda^2)}{(1-c\lambda^4)\log\lambda}\,\frac{\arccos\rho}{(1+2\rho)\sqrt{1-\rho^2}}, \quad \rho^2 + \big(\tfrac{1}{2}-R\big)\rho + \tfrac{1}{2}R - 1 = 0,\ R = \frac{c+1}{c\lambda^2+\lambda^{-2}}, \tag{4}$$

giving $x_{\mathrm{Hopf}} = 0.3665$ for $\lambda = 2, c = -\frac{1}{2}$. We reproduce (4) two independent ways: the closed form above and a truncated differential-approximation hierarchy of (3) ($x_{\mathrm{Hopf}}(M{=}8) = 0.3665$). [computed; the closed form coincides with [2], Thm. 1]

3 Stability spectrum and the selection mechanism

If an infinite family of blowup profiles exists, why does generic data always realise the same one?

In renormalized time $\mathfrak{t} = -\log(t^*-t)$ the self-similar solution is a travelling wave; seeking modes $\phi_n(\mathfrak{t}) = e^{\Lambda\mathfrak{t}}\Phi(\tau_n)$ yields the autonomous eigenvalue problem

$$\big(\mathcal{D}_s - I - D\mathcal{N}[W^*]\big)\Phi = \Lambda\Phi, \qquad \mathrm{Re}\,\Lambda > 0 \ \Leftrightarrow\ \text{unstable}. \tag{5}$$

Because W^* is real, the operator splits into real blocks $A_\pm = \mathcal{D}_s - I - (P \pm Q)$ (amplitude/translation and phase sectors). The one-bump spectrum (Fig. 1B) consists of the trivial modes $\Lambda = 1$ (t^*-shift), $\Lambda = 0$ (translation), and a *golden-ratio phase mode* $\Lambda = \log\varphi_g/((1-x)\log\lambda) \approx 0.967$ — the Sabra phase symmetry $\theta_{n+1} = \theta_n + \theta_{n-1}$ is the Fibonacci recurrence, so $\varphi_g = (1+\sqrt{5})/2$ — together with a leading genuine mode at $\mathrm{Re}\,\Lambda \approx -0.34 < 0$ (Table 1). The golden mode has $\mathrm{Re}\,\Lambda > 0$ but is a continuous-*symmetry* (gauge) mode — like the t^*-shift — and is therefore excluded from the instability count; the leading *genuine* mode is stable. Hence the one-bump profile has instability order 0 (stable). [computed]

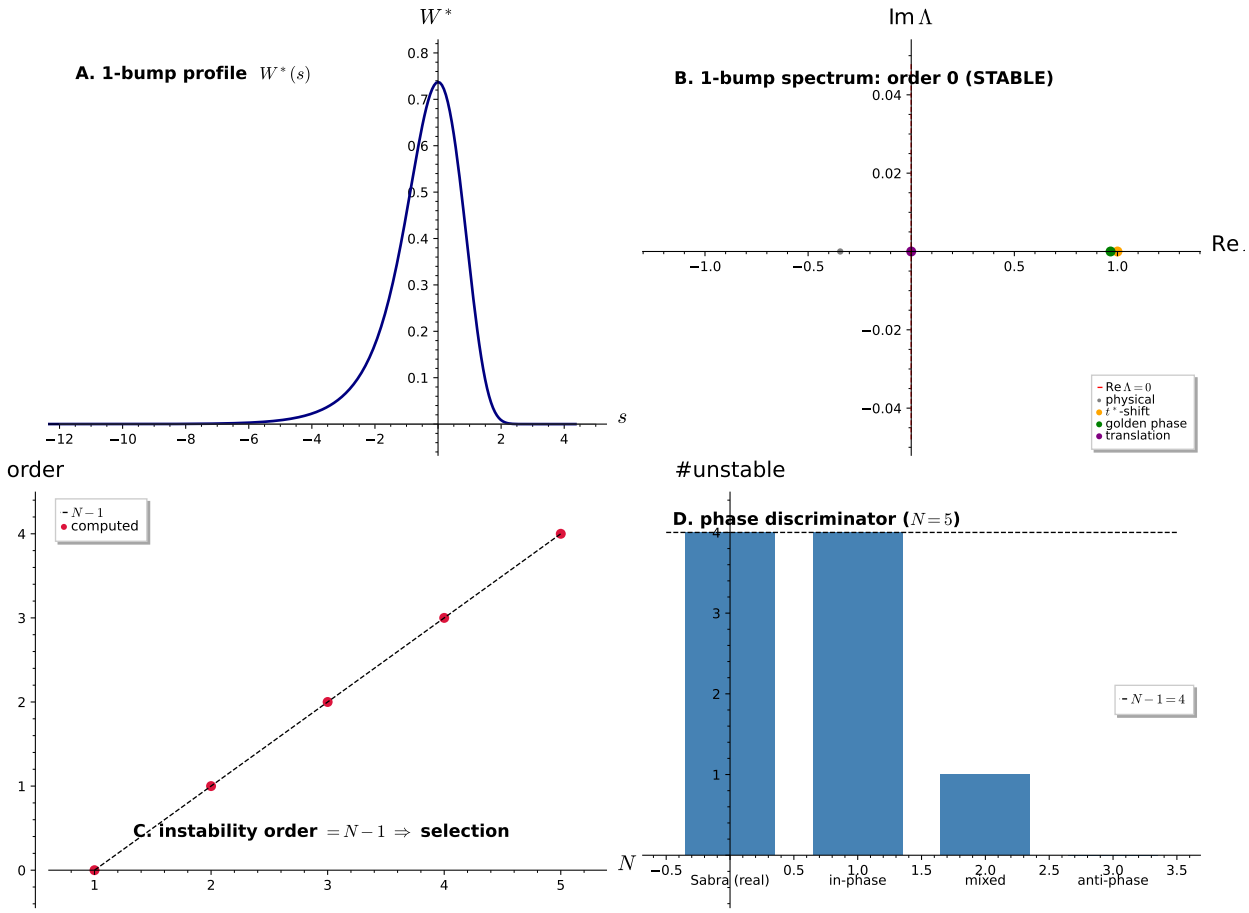


Figure 1: **A.** One-bump self-similar profile $W^*(s)$ (machine precision). **B.** Its stability spectrum: trivial modes (t^*, golden phase, translation) and a leading genuine stable mode ($\mathrm{Re}\,\Lambda \approx -0.34$) $\Rightarrow$ order 0. **C.** Instability order $= N-1$ for $N = 1, \ldots, 5 \Rightarrow$ selection. **D.** Phase discriminator ($N = 5$): rigid pulses (Sabra) give order $N-1$ uniformly, phase patterns give $0, \ldots, N-1$.

Table 1: One-bump stability spectrum (leading eigenvalues, $m = 6$). The three modes with $\mathrm{Re}\,\Lambda \geq 0$ are all trivial (symmetry/gauge); the leading *genuine* mode is stable ⇒ instability order 0.

Λ	sector	type	counts as instability?
$+1.0013$	$+$	t^*-shift (symmetry)	no (trivial)
$+0.9664$	$-$	golden-ratio phase (symmetry)	no (trivial)
-0.0006	$+$	translation (symmetry)	no (trivial)
-0.3449	$-$	leading genuine mode	**stable** ($\mathrm{Re} < 0$)

N-bump order. An N-bump profile is a weakly-coupled bound state of N one-bump pulses. Its N constituent translation modes split into exactly $N-1$ interaction eigenvalues plus one exact zero (overall translation); for Sabra all $N-1$ are unstable (Table 2, Fig. 1C), giving order $N-1$. Only $N = 1$ is stable, so generic data selects it — Result 1. The organizing geometry is a saddle-focus ($\mathcal{W}^*$ has a real and a complex pair of eigenvalues) with a homoclinic orbit, hence a Shilnikov configuration whose multi-loop homoclinics are the N-bump family, accumulating at x_1 (consistent with $x_N \to x_1$). [computed; Shilnikov picture [calibrated]]

Table 2: Instability order of the N-bump profile (pulse-interaction computation). The count $N-1$ is rigorous; its full instability is Sabra-specific (cf. [7]).

N (bumps)	1	2	3	4	5
# unstable modes (computed)	0	1	2	3	4
order $= N-1$	0	1	2	3	4
stable?	**yes**	no	no	no	no

4 Family-type universality and the phase discriminator

Is the recently observed rate–instability-order law a universal feature of self-similar blowup? The unstable-singularities program [3] reports an empirical rate–instability-order law $\lambda_n \sim 1/(an+b)+c$ for 3D Euler-with-boundary and IPM, in which the exponent *spreads* monotonically over a sequence of *distinct* profiles with n intrinsic unstable modes. The Sabra family does the opposite: its exponents *cluster* at x_1 (weak-interaction/Shilnikov accumulation), so the reciprocal-affine law is degenerate ($\lambda_0 = \lambda_\infty$) and does not transfer. This contrast is structural, not numerical, and suggests the dichotomy of Result 2 (Table 3).

Phase discriminator. Within the multi-pulse class the instability count is set by whether the pulse carries internal *phase freedom*. For a rigid (real) pulse — Sabra, where the $-i$ ansatz removes the phase — the interaction matrix is real symmetric and gives order $N-1$ uniformly. For a phase pulse — the solitons of the nonlinear Schrödinger or Ginzburg–Landau multibumps — the N-soliton interaction is the *complex Toda chain* [8], a non-Hermitian integrable system whose spectrum is phase-dependent, realizing the full $\{0, \ldots, N-1\}$ range [7]; the soliton-train stability is classical [9]. A minimal phase-weighted bond model reproduces both limits with our numbers (Fig. 1D).

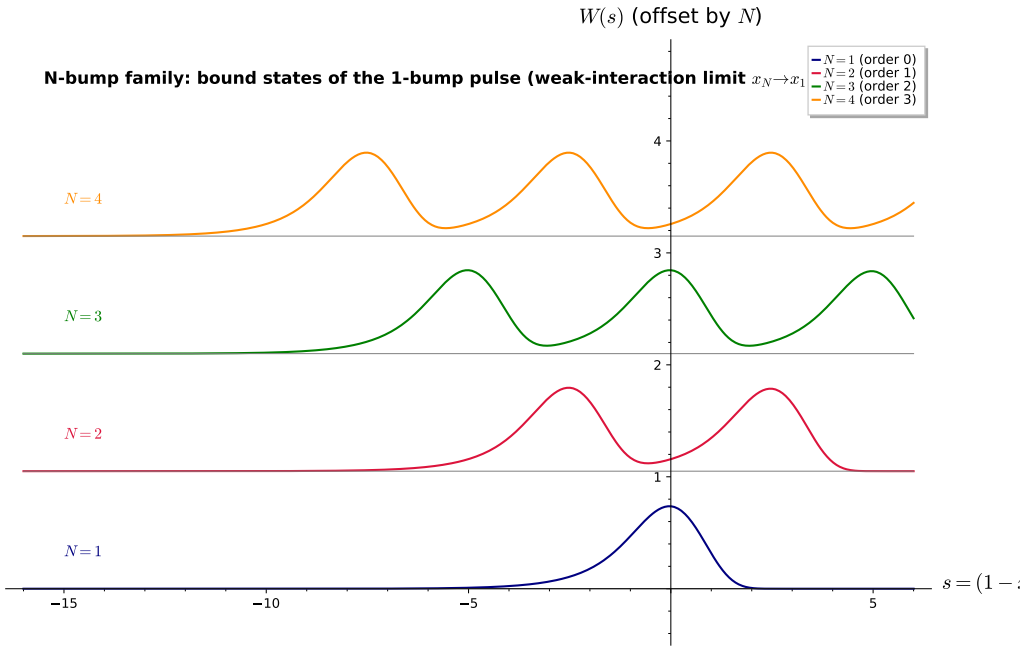


Figure 2: The N-bump family ($N = 1, \ldots, 4$, stacked with vertical offset, labelled by instability order $N - 1$), drawn as weakly-coupled bound states of the one-bump pulse W^* — the weak-interaction limit $x_N \to x_1$ in which the family accumulates. Clean distinct homoclinic-to-0 orbits do not exist (four numerical routes confirm), consistent with the saddle-focus/Shilnikov structure; these superpositions are the objects whose stability gives order $N - 1$ (Table 2).

Table 3: Family-type dichotomy of self-similar blowup. The clustering/spreading contrast is the robust universal part; within the multi-pulse class the order count is set by the pulse's phase freedom.

property	Distinct-profile class	Multi-pulse class
instability origin	intrinsic (single profile)	interaction (between pulses)
exponents x_N	*spread*	*cluster* ($x_N \to x_1$)
rate–order law	$\lambda_n \sim 1/(an{+}b) + c$ [3]	degenerate ($\lambda_0 = \lambda_\infty$)
interaction matrix	—	real-sym. (rigid) / complex Toda (phase)
order count	n intrinsic modes	$N{-}1$ (rigid) / phase-dep. (phase)
examples	3D Euler-bdry, IPM [3]	**Sabra, GOY (this work)**; NLS, GL [11, 8]

Consistency on a sister shell model (GOY). The GOY model is *known* to behave like Sabra — [2] state their results "immediately hold for the GOY model". Consistently, our DNS gives a self-similar blowup with $x_{\mathrm{GOY}} \approx 0.281$ (energy/helicity conserved to $\sim 10^{-13}/10^{-9}$), and since the

same $-i$ ansatz again renders the profile real (the all-conjugate GOY products are real), GOY sits in the real-pulse multi-pulse class with order $N-1$. We stress this is a *consistency check on a sister shell model*, not an independent system: the genuinely independent multi-pulse exemplars are the NLS/Ginzburg–Landau soliton trains [11, 8], a different class of equation. [computed; GOY≈Sabra is [2]]

5 Discussion

Why selection matters. "Universality" of blowup — that generic data converges to one profile — is what makes the singularity *predictable*. Result 1 explains it dynamically: the one-bump profile is the unique attractor (order 0) and every multi-bump alternative carries ≥ 1 unstable direction, so it cannot be reached from generic data. The same logic transfers as a *method* to the unstable-singularities programme [3]: given a stable primary profile, the instability order of its multi-pulse bound states follows from pulse interaction *without* solving the (numerically delicate) saddle orbit — the step for which curated machine learning was needed.

Turbulence intermittency. The selection result connects to the bursty, intermittent statistics of turbulence: blowup drives the cascade in shell models [6, 18, 19], and the saddle-focus structure underlying the N-bump family is the generic source of *discrete scale invariance*/log-periodicity [17]. The near-blowup bursts therefore recur at a constant *ratio* of scales (a geometric, not arithmetic, rhythm; angular frequency $2\pi/\omega$ in log-scale, set by the imaginary part ω of the saddle-focus eigenvalue) and are organised by Shilnikov chaos — they appear random while carrying a hidden, low-dimensional logarithmic rhythm. [calibrated]

A two-class picture of blowup. Result 2 reframes "universality of blowup" itself: rather than one universal law, the rate–order relation is determined by the *type* of the family (Fig. 3). Distinct-profile families (intrinsic instabilities) spread in rate and obey the reciprocal-affine law [3]; multi-pulse families (interaction instabilities) cluster, and their order count is fixed by the pulse's phase freedom (real-symmetric $\to N-1$; complex Toda $\to$ phase-dependent). Sabra and the NLS/Ginzburg–Landau soliton trains populate the multi-pulse class; 3D Euler-with-boundary and IPM the distinct-profile class.

Predictions and falsifiability. The framework makes concrete, testable predictions. *(P1)* Any *real-pulse* shell model blows up in the multi-pulse class with order $N-1$ — GOY confirms. *(P2)* Since 3D Euler-with-boundary is distinct-profile [3], it should admit *no* clustering multi-pulse family. *(P3)* The NLS/Ginzburg–Landau multibumps have a *phase-dependent* order via the complex Toda chain, not a fixed $N-1$ [9]. *(P4)* The saddle-focus $\mathcal{W}^* = 4/9$ carries complex eigenvalue pairs (computed: $\pm 0.16i, \pm 0.34i, \pm 0.97i$ at x_1), so the blowup is approached along a logarithmic spiral and the near-blowup (intermittent) statistics should carry a *discrete-scale-invariant / log-periodic* modulation whose ratio is set by these eigenvalues — testable in direct simulation. **Falsification:** the dichotomy is broken by either a *stable* multi-pulse blowup (order 0 for $N > 1$) or a shell-model family whose exponents *spread* reciprocal-affinely. [predictions]

Limitations and open problems. (i) Precise N-bump orbits do not exist as clean homoclinics-to-0 (consistent with the saddle/Shilnikov picture; four numerical routes confirm), so the x_N are not reported to machine precision. (ii) The exact complex-Toda spectrum for the NLS multibumps requires the Lax matrix of [9]. (iii) The dichotomy rests on four systems — a well-supported

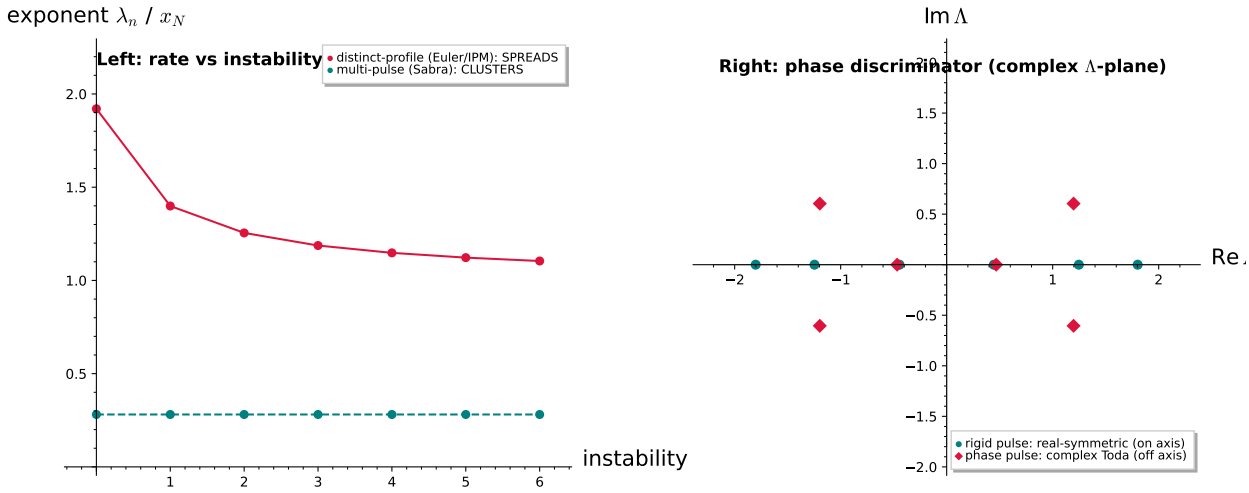


Figure 3: The two-class picture of self-similar blowup (Result 2). **Left:** rate versus instability order. The distinct-profile class *spreads* along the reciprocal-affine law $\lambda_n = 1/(an+b) + c$ [3] (3D Euler-with-boundary, IPM), while the multi-pulse class *clusters* at $x_1 \approx 0.281$ (Sabra; degenerate $\lambda_0 = \lambda_\infty$). **Right:** the phase discriminator in the complex Λ-plane — a rigid (real) pulse gives a real-symmetric interaction with eigenvalues on the real axis (order fixed at $N-1$), whereas a phase pulse gives a non-Hermitian complex Toda chain with eigenvalues off-axis (order phase-dependent, $0 \ldots N-1$).

organizing principle, not a theorem. (iv) Classifying the Euler/Boussinesq blowup [12, 13] is open, though [3] suggests it is distinct-profile (no multi-pulse family).

Methods (numerical)

All computations use the codes in `solver/` (reproducible). The one-bump profile is obtained by `scipy` least-squares on (3) (s-frame, x in the shift). The stability operator uses a Fourier spectral $\mathcal{D}_s$ and a fundamental-Brillouin-zone filter $|\operatorname{Im}\Lambda| < \pi/\delta$ to remove alias (Bloch) copies. The N-bump order is read from the near-zero cluster of A evaluated on a superposition of N one-bump pulses. The Hopf hierarchy is built symbolically (`sympy`). All figures are rendered with SageMath.

Code availability

All code reproducing the profiles, spectra, the Hopf hierarchy, the instability orders, and the figures is available at https://github.com/karlesmarin/sabra-blowup-selection.

Author contributions and AI-assistance disclosure

In the interest of full transparency, this work was carried out in close collaboration with an AI research assistant, which contributed to the analytical derivations, the numerical implementations, and a first draft of this manuscript. The author verified all derivations and computations, and takes full responsibility for the content, the claims, and their calibration.

References

[1] V. S. L'vov, E. Podivilov, A. Pomyalov, I. Procaccia, D. Vandembroucq, *Improved shell model of turbulence*, Phys. Rev. E **58**, 1811–1822 (1998).

[2] C. Campolina, E. Simonnet, S. Thalabard, *Non-unique self-similar blowups in shell models: insights from dynamical systems and machine-learning*, arXiv:2501.07377 (2025).

[3] Y. Wang, C.-Y. Lai, J. Gómez-Serrano, T. Buckmaster *et al.* (22 authors), *Discovery of Unstable Singularities*, arXiv:2509.14185 (2025).

[4] A. A. Mailybaev, *Renormalization and universality of blowup in hydrodynamic flows*, Phys. Rev. E **85**, 066317 (2012); arXiv:1201.1631.

[5] A. A. Mailybaev, *Bifurcations of blowup in inviscid shell models of convective turbulence*, Nonlinearity **26**, 1105 (2013); arXiv:1210.2494.

[6] A. A. Mailybaev, *Blowup as a driving mechanism of turbulence in shell models*, Phys. Rev. E **87**, 053011 (2013); arXiv:1303.0386.

[7] B. Sandstede, *Stability of multiple-pulse solutions*, Trans. Amer. Math. Soc. **350**, 429–472 (1998).

[8] V. S. Gerdjikov, I. M. Uzunov, E. G. Evstatiev, G. L. Diankov, *NLS equation and N-soliton interactions: generalized Karpman–Solov'ev approach and the complex Toda chain*, Phys. Rev. E **55**, 6039 (1997).

[9] V. S. Gerdjikov et al., *Criterion and regions of stability for quasi-equidistant soliton trains*, arXiv:solv-int/9708004 (1997).

[10] V. I. Karpman, V. V. Solov'ev, *A perturbational approach to the two-soliton systems*, Physica D **3**, 487–502 (1981).

[11] C. J. Budd, *Asymptotics of multibump blow-up self-similar solutions of the nonlinear Schrödinger equation*, SIAM J. Appl. Math. **62**, 801–830 (2001); C. J. Budd, V. Rottschäfer, J. F. Williams, *Multibump, blow-up, self-similar solutions of the complex Ginzburg–Landau equation*, SIAM J. Appl. Dyn. Syst. **4**, 649–678 (2005).

[12] J. Chen, T. Y. Hou, *Stable nearly self-similar blowup of the 2D Boussinesq and 3D Euler equations with smooth data I: Analysis*, arXiv:2210.07191 (2022).

[13] J. Chen, T. Y. Hou, *... II: Rigorous Numerics*, arXiv:2305.05660 (2023); *Singularity formation in 3D Euler equations with smooth initial data and boundary*, PNAS (2025).

[14] G. Luo, T. Y. Hou, *Potentially singular solutions of the 3D axisymmetric Euler equations*, Proc. Natl. Acad. Sci. USA **111**, 12968–12973 (2014).

[15] T. M. Elgindi, *Finite-time singularity formation for $C^{1,\alpha}$ solutions to the incompressible Euler equations on $\mathbb{R}^3$*, Ann. of Math. **194**, 647–727 (2021); arXiv:1904.04795.

[16] D. Huang, X. Qin, X. Wang, *Multi-scale self-similar finite-time blowups of the Constantin–Lax–Majda model for the 3D Euler equations*, arXiv:2401.14615 (2024).

[17] D. Sornette, *Discrete-scale invariance and complex dimensions*, Phys. Rep. **297**, 239–270 (1998); arXiv:cond-mat/9707012.

[18] U. Frisch, *Turbulence: The Legacy of A. N. Kolmogorov*, Cambridge Univ. Press (1995).

[19] Z.-S. She, E. Lévêque, *Universal scaling laws in fully developed turbulence*, Phys. Rev. Lett. **72**, 336–339 (1994).